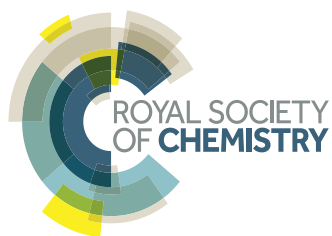
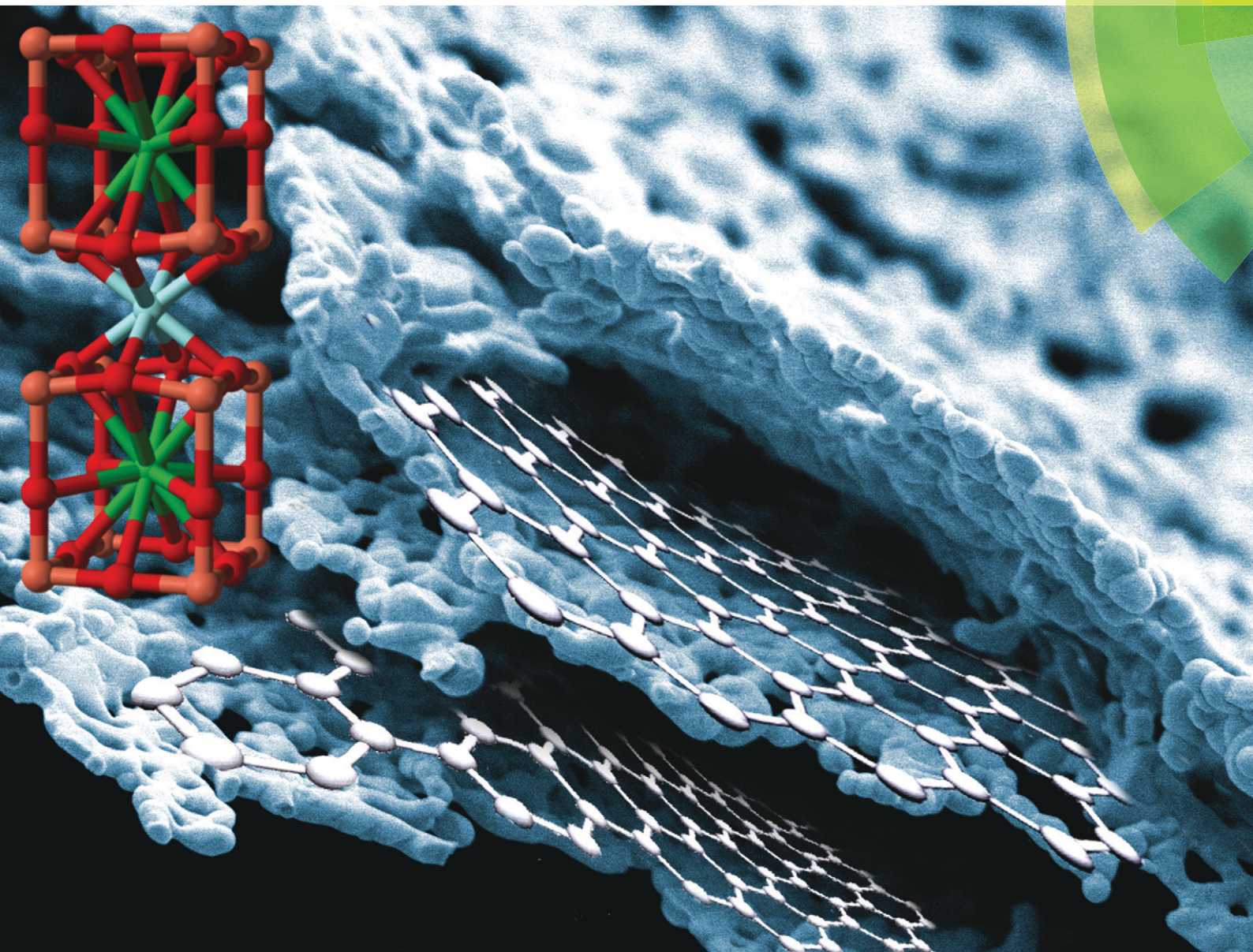


# CrystEngComm

[www.rsc.org/crystengcomm](http://www.rsc.org/crystengcomm)



ROYAL SOCIETY  
OF CHEMISTRY

COMMUNICATION

S. R. Hall *et al.*

Graphene oxide as a template for a complex functional oxide



Cite this: *CrystEngComm*, 2015, 17, 6094

Received 11th May 2015,  
Accepted 5th June 2015

DOI: 10.1039/c5ce00922g

www.rsc.org/crystengcomm

## Graphene oxide as a template for a complex functional oxide†

R. Boston,<sup>‡ab</sup> A. Bell,<sup>‡b</sup> V. P. Ting,<sup>c</sup> A. T. Rhead,<sup>d</sup> T. Nakayama,<sup>e</sup> C. F. J. Faul<sup>b</sup> and S. R. Hall<sup>\*b</sup>

We report the first use of graphene oxide (GO) as a sacrificial template for the structural direction of complex oxides. The superconductor yttrium barium copper oxide (YBCO) was used as a quaternary oxide test system, with the GO templates being used to create foams and layered paper-like structures which retained the superconducting properties of YBCO.

The templated synthesis of inorganic materials is an actively researched field,<sup>1,2</sup> with materials for applications such as piezoelectrics,<sup>3</sup> solid oxide fuel cells<sup>4</sup> and photonic crystals<sup>5</sup> all being created using this flexible and wide-ranging technique. The use of biologically-derived templates has yielded a number of hitherto unavailable morphologies in complex oxide materials, such as nanowires,<sup>6,7</sup> microspheres,<sup>8</sup> and more complex structures.<sup>9</sup> Template-based synthesis pathways have also given greater insight into the fundamental mechanisms that govern nanoscale crystal growth.<sup>10</sup> Typically highly carbonaceous and strongly chelating, these templates prevent agglomeration and sintering of stable intermediates during high temperature syntheses. This allows the formation of the desired phase without slow and energy-intensive heating and grinding steps.<sup>11</sup> Thus, templated syntheses are more efficient, whilst still allowing for fine control of phase and morphology.

Whilst nano- and micrometre-scale growth of crystallites using biotemplates is well understood, it is challenging to up-scale this control to create well-ordered macroscopic

structures. This is possible by use of a sacrificial template, which directs the morphology at the chosen length scale<sup>12,13</sup> and is destroyed during synthesis, leaving the final inorganic product as a polycrystalline replica.<sup>14,15</sup> This allows, for example, construction of monolithic inverse opaline crystals from simple oxides such as SiO<sub>2</sub> and TiO<sub>2</sub><sup>16</sup> or metals.<sup>17</sup> There are many prior examples of simple oxides constructed from sacrificial templates, but their use for ternary or quaternary materials, such as complex metal oxides like YBa<sub>2</sub>Cu<sub>3</sub>O<sub>7-δ</sub> (Y123), remains relatively rare.<sup>18–21</sup> Y123 is an excellent model system for testing the efficacy of templating methods in complex oxides due to the strong dependence of the superconducting properties of Y123 upon the templated morphology and phase purity.

Graphene oxide (GO) is a promising material for templating metal oxides, showing effective templating of SiO<sub>2</sub> into a nanoflake morphology.<sup>22</sup> GO consists of single-atom-thick carbon sheets, but differs markedly from graphene. GO contains a random oxygen-rich network of sp<sup>3</sup>-hybridised carbon atoms, interspersed with islands of pristine sp<sup>2</sup>-hybridised graphitic carbon<sup>23,24</sup> (from which GO is initially synthesized). GO is well-known for its flexibility for the creation of different structures such as three-dimensional macroporous solids,<sup>25,26</sup> hydrogels,<sup>27</sup> and papers.<sup>28</sup> As GO starts from an aqueous dispersion, it is able to take on the shape of the vessel in which it is prepared, making it extremely versatile for the creation of bespoke shapes, for example curved structures or porous monoliths. It is also capable of uptake of transition metal ions (for example Cu<sup>2+</sup>) from solution.<sup>29</sup> The wide variety of available final morphologies from a single material,<sup>30</sup> combined with an abundance of chelating hydroxyl and ketone functionalities,<sup>24,31</sup> makes GO attractive for use as a template for oxide materials.

Here we present the first instance of GO-templating of a quaternary metal oxide and demonstrate the use of monolithic GO templates to produce, in this case, the complex oxide Y123. Two morphologies of GO (foam and paper) were chosen; both were synthesized from GO aqueous solutions by previously reported methods<sup>25,28</sup> and were successfully used

<sup>a</sup> Bristol Centre for Functional Nanomaterials, Centre for Nanoscience and Quantum Information, University of Bristol, Tyndall Avenue, Bristol BS8 1FD, UK

<sup>b</sup> School of Chemistry, University of Bristol, Cantock's Close, Bristol, BS8 1TS, UK. E-mail: simon.hall@bristol.ac.uk

<sup>c</sup> Department of Chemical Engineering, University of Bath, Bath, BA2 7AY, UK

<sup>d</sup> Department of Mechanical Engineering, University of Bath, Bath, BA2 7AY, UK

<sup>e</sup> Department of Electrical Engineering Nagaoka University of Technology, 1603 1 Kamitomioka, Nagaoka, Niigata, 940 2188, Japan

† Electronic supplementary information (ESI) available: Full experimental details, TEM, electron diffraction, powder XRD, and critical current density plots. See DOI: 10.1039/c5ce00922g

‡ These authors contributed equally.





to control and direct the growth of highly crystalline superconducting Y123 structures with highly porous, or oriented structures, respectively. The resulting Y123 materials demonstrate an improvement in critical current density of the superconducting phase when compared with solid-state syntheses,<sup>32,33</sup> and act as proof-of-concept that GO can be used as a template for complex oxides.

Full details of the experimental methods can be found in the supporting information, but briefly, monolithic GO structures with foam and layered paper-like microstructure were immersed in aqueous solutions of Y, Ba, and Cu nitrate salts. Soaked templates were then dried and calcined to obtain templated YBCO. Initially the structure of the template and inorganic replicas were investigated using SEM, as shown in Fig. 1. Fig. 1a and b show SEM micrographs of the GO foam and paper respectively, prior to soaking in the precursor, with inset photographs showing the macroscopic monoliths. SEM micrographs of the two templated solid structures (Fig. 1c–f) show excellent retention of the templates' porous (foam) and

highly layered (paper) structures, respectively. The templated products show a polycrystalline structure, arranged in the same morphology and microstructure as the GO templates.

Non-destructive imaging by X-ray micro-computed tomography (X-ray  $\mu$ -CT) revealed an interconnected macroporous internal structure (Fig. 2). Fig. 2a shows a model of the macropores present within a small section of the Y123 foam, with Fig. 2b showing a cut-away of the sample illustrating the micron-scale porous internal structure. This structure is a good replica of the GO template, and indicates that the porous structure is retained throughout the sample during calcination. The pore mapping was used to obtain an average porosity of 42%. The structure of the paper-like Y123 is displayed in Fig. 2c, with Fig. 2d showing the layered structure is present throughout the sample, imparted by the GO template.

The composition of both the foam- and paper-templated Y123 was determined using TEM/EDX (Fig. S1†) and powder X-ray diffraction (Fig. S2†). The majority phase in both the foam and paper materials (Fig. S2a and b† respectively) is  $\text{YBa}_2\text{Cu}_3\text{O}_{6.9}$  (JCPDS card 79-0653), which is consistent with optimal oxygenation. A small number of impurity phases were also observed, including  $\text{CuO}$ ,  $\text{BaCuO}_2$  and  $\text{Y}_2\text{BaCuO}_5$ .

Central to the success of any templated system is the mechanism by which the template acts to produce the final product (in this case Y123). This can be considered in two ways: the chemical pathway and the physical direction of crystallites imparted by the template. The chemical pathway for the formation of Y123 was investigated with a series of increasing calcination temperatures. Fig. 3 shows the indexed PXRD patterns of samples heated to temperatures between 200 °C and 900 °C (at 100 °C intervals) and suggests that this synthesis proceeds *via* a different low-temperature pathway to that which has been observed previously with some polysaccharide biotemplates.<sup>10–12</sup> The synthesis does, however, show some similarities to the high carbon-content dextran-based syntheses,<sup>8</sup> as might be expected given the high carbon content of GO.

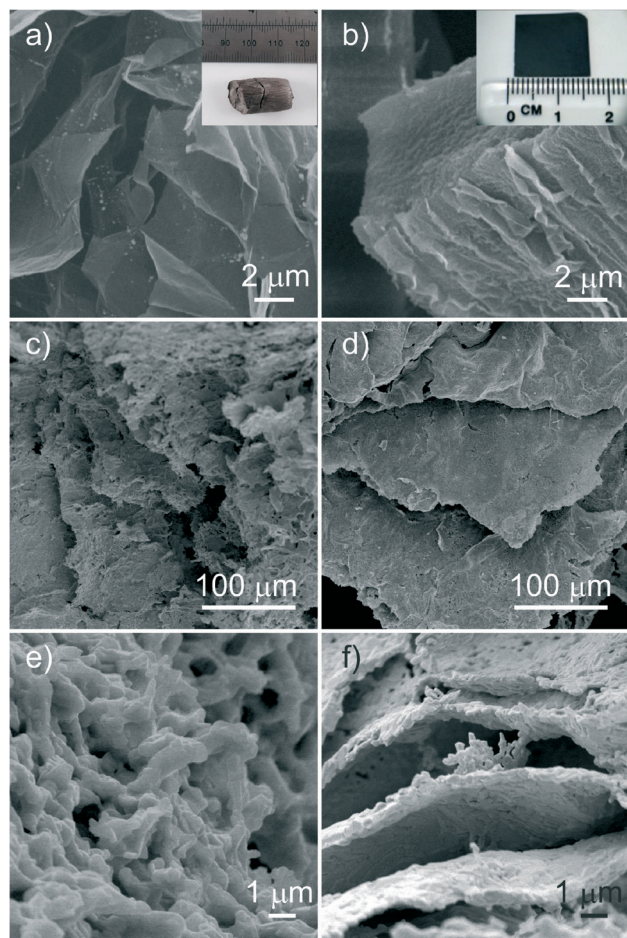


**Fig. 1** SEM micrographs of a) foam and b) paper templates prior to combination with the precursor solution, with inset photographs of each. c) and d) show micrographs of the calcined Y123 foam and layered structure respectively, with the microstructures shown in e) and f). The macroscopic structure of the GO is retained between the uncalcined (a and b) and calcined samples (c–f), in particular the layers in the GO paper which can be clearly seen in d and f.

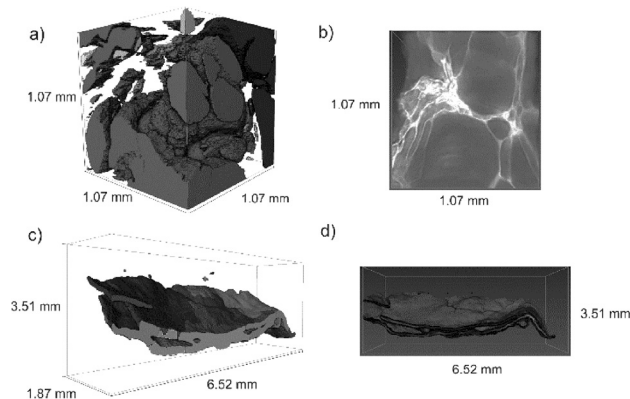


**Fig. 2** X-ray  $\mu$ -CT images of a) and b) the Y123 foam showing, respectively, internal macro-pore structure and solid pore walls, and c) and d) the Y123 paper showing, respectively, internal layered structure and detailed morphology.



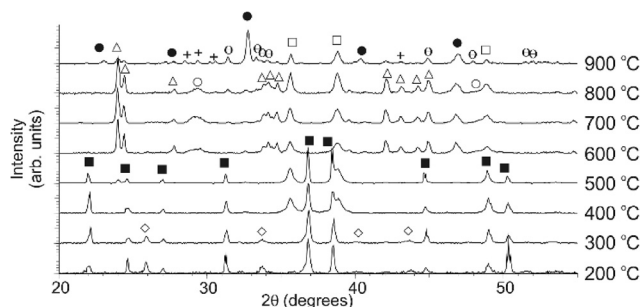


**Fig. 3** Temperature study of the formation of the Y123 phase. Phases present are  $\text{Ba}(\text{NO}_3)_2$  (■),  $\text{Cu}(\text{NO}_3)_2(\text{H}_2\text{O})_3$  (◊),  $\text{YBa}_2\text{Cu}_3\text{O}_{6.9}$  (●),  $\text{CuO}$  (□),  $\text{BaCO}_3$  (Δ),  $\text{Y}_2\text{O}_3$  (○),  $\text{BaCuO}_2$  (+) and  $\text{Y}_2\text{Cu}_2\text{O}_5$  (θ).

At 200 °C, the major crystalline phases present are the precursor materials barium and copper nitrates (JCPDS cards 76-1376 and 45-0594 respectively). As fully chelated ions are non-crystalline and therefore do not appear in the XRD pattern, the presence of these crystalline phases at these low temperatures is due to recrystallization of excess precursor solution present on the surface of the template upon drying. Barium nitrate is observed in greater quantities than the other two nitrates due to the fact that yttrium nitrate thermally decomposes below 200 °C, and copper nitrate between 200 °C and 300 °C (accounting for the small quantities observed at these temperatures).

Between 300 °C and 400 °C the copper ions chelated in the monolith react with the template to form copper(II) oxide (JCPDS card 74-1021) which, crucially, allows for the retention of the template structure while the desired inorganic phase forms. Between 400 °C and 600 °C, as the template fully decomposes, the  $\text{Ba}^{2+}$  and  $\text{Y}^{3+}$  ions react to form yttrium oxide and barium carbonate (JCPDS cards 74-1828 and 41-0373 respectively), which are homogeneously spread throughout the material.

The next significant change in the sample occurs in the 800 °C and 900 °C interval, where a solid–solid reaction between  $\text{Y}^{3+}$ ,  $\text{Ba}^{2+}$  and  $\text{Cu}^{2+}$  ions occurs due to the decomposition of  $\text{BaCO}_3$  above 811 °C. Here again, the fact that the template is perfectly replicated indicates that the reaction to form the final product is occurring in the solid state, and as is observed in templates such as dextran,<sup>21</sup> the final Y123 product only forms where the template has been. In this templated approach, however, the time over which this reaction occurs is reduced to two hours due to the higher degree of mixing between the three precursor ions within by the chelating template. The synthesis then proceeds as observed previously in typical biotemplated systems,<sup>8,34</sup> with Y123 emerging as the major phase between 800 °C and the final calcination temperature, 920 °C. Small quantities of  $\text{Y}_2\text{Cu}_2\text{O}_5$  (JCPDS card 33-0511) and  $\text{BaCuO}_2$  (JCPDS card 70-0441) are also observed at 900 °C, indicating that the final formation of the Y123 phase is dependent on both the higher final temperature (920 °C) and a longer hold time than was used in the temperature study. By holding the samples at 920 °C for

two hours, the quantity of these small impurity phases were reduced (Fig. S2†).

SQUID magnetometry of the templated Y123 was performed to determine the transition temperature,  $T_c$  (Fig. 4) and critical current density,  $J_c$  (Fig. S3†) of the templated Y123. Transition temperatures of  $90 \pm 1$  K and  $89 \pm 1$  K were measured for the foam and paper morphologies, respectively, close to the optimum value for  $T_c$  in Y123. The critical current densities were determined at 1T applied field and 10 K. Values were measured to be  $0.10 \text{ MA cm}^{-2}$  (foam) and  $0.05 \text{ MA cm}^{-2}$  (layered). The difference between values the foam and paper-like samples can be attributed to the greater continuity of the crystallites in the foam sample; the greater number of interconnects between crystallites results in there being more pathways in which the supercurrent can flow, resulting in a larger critical current density being measured. Conversely the paper-like structure, being composed of layers, has these same crystallite connections in only two dimensions, resulting in a lower value measured for  $J_c$ .

These values are greater than previously reported values of  $J_c$  for commercially available polycrystalline Y123, which are of the order  $0.02 \text{ MA cm}^{-2}$ .<sup>21</sup> Whilst the values obtained are lower than those known for some Y123 syntheses<sup>35</sup> we believe the templated synthesis technique presented here has the advantage of allowing customization of the morphology

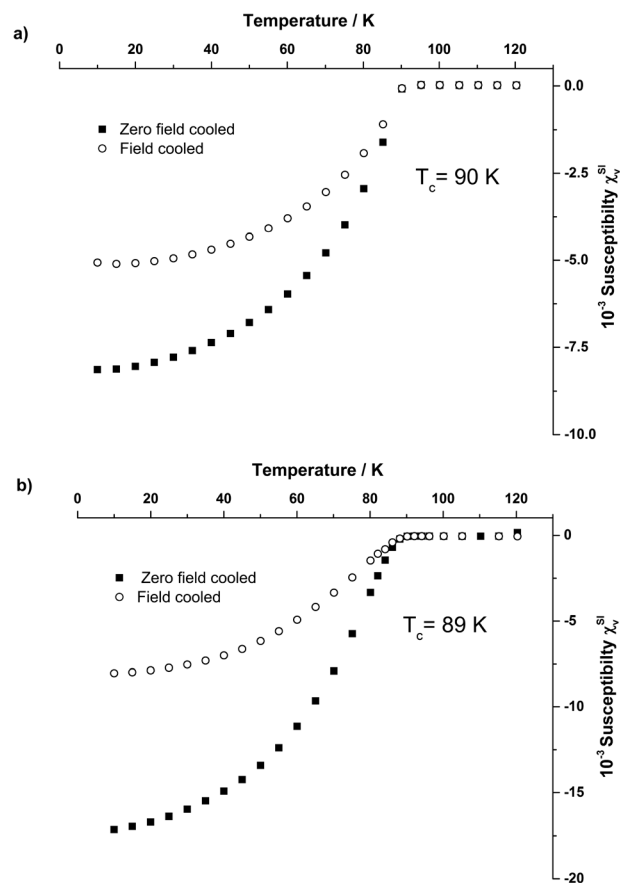


**Fig. 4** SQUID magnetometry showing superconducting transition temperature,  $T_c$ , of a) Y123 foam and b) paper Y123.



of quaternary metal oxides such as YBCO to suit specific applications, while maintaining a good material quality.

In conclusion, we have successfully exploited a novel and highly modifiable template for the construction of oxide materials with pre-determined micro-scale structure, illustrated by the creation of superconducting oxide monoliths. We have shown that, due to low temperature stable intermediate phase formation, the final product faithfully retains the structure of the uncalcined GO template, allowing porous foams and highly layered oxide structures to be created. With many further GO morphologies possible, this template has potential for great utility in obtaining application-specific morphologies, *e.g.* foams for rapid access of cryogenics to improve cool-down times in superconductors, which retain the desired properties. We have also elucidated the crystallochemical mechanism by which templates allow formation of the Y123 phase. This work demonstrates that GO deserves a place alongside biotemplates in the arsenal of options available for creating highly ordered functional inorganic materials.

## Data accessibility

Original TEM and SEM images and raw data from XRD, X-ray micro-CT and SQUID magnetometry pertaining to all materials in this manuscript have been placed in the University of Bristol Research Data Repository ([www.data.bris.ac.uk/data/](http://www.data.bris.ac.uk/data/)).

## Acknowledgements

AB, RB and SRH acknowledge the Engineering and Physical Sciences Research Council (EPSRC), UK (grant EP/G036780/1), and, RB and SRH the Bristol Centre for Functional Nanomaterials for project funding. All authors would like to acknowledge the Electron and Scanning Probe Microscopy Facility at the School of Chemistry, University of Bristol for the use of electron microscopes. VPT thanks the University of Bath for funding via a Prize Fellowship. CFJF thanks the University of Bristol for support.

## Notes and references

- 1 Z. Schnepf, *Angew. Chem., Int. Ed.*, 2013, 52, 1096.
- 2 H. Zhou, T. Fan and D. Zhang, *ChemSusChem*, 2011, 4, 1344.
- 3 Z. Schnepf, J. Mitchells, S. Mann and S. R. Hall, *Chem. Commun.*, 2010, 46, 4887.
- 4 D. Dong, Y. Wu, X. Zhang, J. Yao, Y. Huang, D. Li, C.-Z. Li and H. Wang, *J. Mater. Chem.*, 2011, 21, 1028.
- 5 M. J. Jorgensen and M. H. Bartl, *J. Mater. Chem.*, 2011, 21, 10583.
- 6 K. Cung, B. J. Han, T. D. Nguyen, S. Mao, Y.-W. Yeh, S. Xu, R. R. Naik, G. Poirier, N. Yao, P. K. Purohit and M. C. McAlpine, *Nano Lett.*, 2013, 13, 6197.
- 7 M.-Y. Chang, W.-H. Wang and Y.-C. Chung, *J. Mater. Chem.*, 2011, 21, 4966.
- 8 R. Boston, A. Carrington, D. Walsh and S. R. Hall, *CrystEngComm*, 2013, 15, 3763.
- 9 J. M. Galloway, J. P. Bramble, A. E. Rawlings, G. Burnell, S. D. Evans and S. Staniland, *Small*, 2012, 8, 204.
- 10 R. Boston, Z. Schnepf, Y. Nemoto, Y. Sakka and S. R. Hall, *Science*, 2014, 344, 623.
- 11 A. Dermont, M. S. Dyer, R. Sayers, M. F. Thomas, M. Tsiamtsouri, H. N. Niu, G. R. Darling, A. Daoud-Aladine, J. B. Claridge and M. J. Rosseinsky, *Chem. Mater.*, 2010, 22, 6598.
- 12 T. T. Vu and G. Marb n, *Applied Catalysis B: Environmental*, 2014, 152–3, 51.
- 13 M. K. Mayeda, J. Hayat, T. H. Epps and J. Lauterbach, *J. Mater. Chem. A*, 2015, 3, 7822.
- 14 R. Banerjee, H. Furukawa, D. Britt, C. Knobler, M. O'Keeffe and O. M. Yaghi, *J. Am. Chem. Soc.*, 2009, 131, 3875.
- 15 A. A. Voskanyan, C.-Y. V. Li, K.-Y. Chan and L. Gao, *CrystEngComm*, 2015, 17, 2620.
- 16 G. I. N. Waterhouse and M. R. Waterland, *Polyhedron*, 2007, 26, 356.
- 17 K. M. Kulinowski, P. Jiang, H. Vaswani and V. L. Colvin, *Adv. Mater.*, 2000, 12, 833.
- 18 E. Culverwell, S. C. Wimbush and S. R. Hall, *Chem. Commun.*, 2008, 1055.
- 19 D. C. Green, M. R. Lees and S. R. Hall, *Chem. Commun.*, 2013, 49, 2974.
- 20 E. S. Reddy, J. G. Noudem and C. Goupil, *Energy Convers. Manage.*, 2007, 48, 1251.
- 21 D. Walsh, S. C. Wimbush and S. R. Hall, *Chem. Mater.*, 2007, 19, 647.
- 22 Z. Lu, J. Zhu, D. Sim, W. Zhou, W. Shi, H. H. Hng and Q. Yan, *Chem. Mater.*, 2011, 23, 5293.
- 23 A. Lerf, H. He, M. Forster and J. Klinowski, *J. Phys. Chem. B*, 1998, 102, 4477.
- 24 K. Erickson, R. Erni, Z. Lee, N. Alem, W. Gannett and A. Zettl, *Adv. Mater.*, 2010, 22, 4467.
- 25 L. Qiu, J. Z. Liu, S. L. Y. Chang, Y. Wu and D. Li, *Nat. Commun.*, 2012, 3, 1241.
- 26 J. L. Vickery, A. J. Patil and S. Mann, *Adv. Mater.*, 2009, 21, 2180.
- 27 H. Bai, C. Li, X. Wang and G. Shi, *Chem. Commun.*, 2010, 46, 2376.
- 28 D. A. Dikin, S. Stankovich, E. J. Zimney, R. D. Piner, G. H. B. Dommett, G. Evmenenko, S. T. Nguyen and R. S. Ruoff, *Nature*, 2007, 448, 457.
- 29 X. Mi, G. Huang, W. Xie, W. Wang, Y. Liu and J. Gao, *Carbon*, 2012, 50, 4856.
- 30 H.-P. Cong, J.-F. Chen and S.-H. Yu, *Chem. Soc. Rev.*, 2014, 43, 7295.
- 31 A. M. Dimiev, L. B. Alemany and J. M. Tour, *ACS Nano*, 2013, 7, 576.
- 32 H. S zeri, H.  zkan and N. Ghazanfari, *J. Alloys Compd.*, 2007, 428, 1.
- 33 A. Usoskin, J. Dzick, A. Issaev, J. Knoke, F. Garc a, F. Garc a-Moreno, K. Sturm and H. C. Freyhardt, *Supercond. Sci. Technol.*, 2001, 14, 676.
- 34 D. Larbalestier, A. Gurevich, D. M. Feldmann and A. Polyanskii, *Nature*, 2001, 414, 368.
- 35 Z. A. C. Schnepf, S. C. Wimbush, S. Mann and S. R. Hall, *Adv. Mater.*, 2008, 20, 1782.

